Available online at www.sciencedirect.com

ScienceDirect

journal homepage: www.elsevier.com/locate/ajps

Original Research Paper

Preparation of slab-shaped lactose carrier particles for dry powder inhalers by air jet milling

Xiang Kou [a,b], *Lai Wah Chan* [a], *Changquan Calvin Sun* [b,*], *Paul Wan Sia Heng* [a,**]

[a] *GEA-NUS Pharmaceutical Processing Research Laboratory, Department of Pharmacy, National University of Singapore, 18 Science Drive 4, Singapore 117543, Singapore*

[b] *Pharmaceutical Materials Science and Engineering Laboratory, Department of Pharmaceutics, University of Minnesota, 308 Harvard St. SE, Minneapolis, MN 55455, USA*

ARTICLE INFO

Article history:
Received 14 May 2016
Received in revised form 27 August 2016
Accepted 4 September 2016
Available online 21 September 2016

Keywords:
Particle engineering
Shape modification
Lactose
Dry powder inhaler

ABSTRACT

Dry powder inhalers are often formulated by attaching micronized drug particles onto carrier particles, which are generally lactose. In this study, commercially available lactose was air jet milled to produce unique slab-like coarse carrier particles, which have larger and rougher surfaces compared to other commercially available lactose. Two key processing factors, i.e., classifier speed and jet milling pressure, were systematically investigated. The largest fraction of slab-like particles in the resulting powder was obtained at a classifier speed of 3000 rpm. The slab-like coarse carrier particles are expected to exhibit superior performance than commercial lactose due to their unique surface properties.

1. Introduction

Particle engineering is an important strategy for solving problems in drug delivery by dry powder inhaler (DPI). Lactose in the size range of 20–100 μm is usually used as coarse carrier in DPI formulations [1]. In this size range, the flowability of the powder is optimal leading to a better DPI performance [2]. Besides size and size distribution, particle shape is also important because it can influence not only powder flow [3] but

* *Corresponding author.* Pharmaceutical Materials Science and Engineering Laboratory, Department of Pharmaceutics, University of Minnesota, 9-127B Weaver-Densford Hall, 308 Harvard Street S.E., Minneapolis, MN 55455, USA. Fax: 001-612-626-2125.
E-mail address: sunx0053@umn.edu (C.C. Sun).
** *Corresponding author.* GEA-NUS Pharmaceutical Processing Research Laboratory, Department of Pharmacy, National University of Singapore, 18 Science Drive 4, Singapore 117543, Singapore. Fax: +65 6779 1554.
E-mail address: paulheng@nus.edu.sg (P.W.S. Heng).
Peer review under responsibility of Shenyang Pharmaceutical University.
http://dx.doi.org/10.1016/j.ajps.2016.09.002

also the performance of a formulation [4]. Irregularly shaped particles, such as needle shape, are superior to more isodimensional particles for DPI [5]. Surface roughness can also affect the performance by modifying the available contact area of the carrier [6]. In the literature, there is a wealth of information on the production of spherical shaped particle [7,8] but only a paucity of information on how to produce irregular shaped particles, such as needle or slab-shaped particles. Irregular shaped particles were mainly produced by controlled crystal growth in a solution, often in different solvent systems [9–15] or by changing crystallization parameters [16], sometimes aided by the addition of additives [17–19]. Sonocrystallization was also successfully used to prepare needle-shaped crystals of both excipients [20–22] and APIs [23]. The disadvantage of utilizing solution crystallization is the potential complexity in polymorph control [24]. In addition, it often requires several trials to arrive at a suitable solvent system, if that could ever be achieved. Surface roughness modifications were only achieved by mechanofusion and partial recrystallization [25]. Most importantly, those methods, although useful, have several disadvantages that make them difficult to scale-up. Hence, a simple dry particle engineering process for generating irregularly shaped particles is highly desirable.

Jet milling is a well-established method for producing particles in the range of 1–5 μm for many organic crystals. However, it has been largely overlooked as a possible process for producing 20–100 μm particles. Lactose is the most commonly used carrier in pharmaceutical industry for DPI. We hypothesize that fracture of lactose crystals along energetically preferred crystallographic planes during jet milling could modify the typical tomahawk shape of lactose particles and produce novel irregular shape particle. The purpose of this study was to test this hypothesis and identify optimum jet milling parameters for commercial manufacturing of such lactose particles.

2. Materials and methods

2.1. *Preparation of materials*

Commercial lactose (Lactose 100M; Pharmatose 100M, DMV, Veghel, The Netherlands) was used as a model material. Lactose 100M was used to produce powders in the size range of 20–100 μm using an air jet sieve (Hosokawa Micron, Summit, NJ, USA) with sieve aperture sizes of 45 μm and 105 μm, referred as LA-100M. The sieving time for each sieve was 180 s, and the vacuum pressure was set at 30–35 cm water.

A fluidized bed opposed jet mill (AFG 100, Hosokawa, Augsburg, Germany) has 3 modules: classifier, grind milling, and air jet milling. The classifier is to sort the size of the particles, allowing only the desired size particles to pass through for collection. Lactose 100M was classified using the classifier at various classifying wheel speeds. Coarse particles with the size fraction equivalent to the sieved coarse carrier were obtained and referred as LC-100M. Lactose 100M was also milled using the classified grind milling function at various classifying wheel speeds. Again, the size fraction equivalent to the sieved coarse particle was obtained and the product was labeled as LG-100M. The experimental conditions are listed in Table 1.

Table 1 – Experimental conditions for conventional particles.

Batch	Method	Lactose grade	Classifier speed (rpm)
LA-100M	Air jet sieving	100M	–
LC-100M-4K	Classifying	100M	4000
LC-100M-3K	Classifying	100M	3000
LC-100M-2K	Classifying	100M	2000
LG-100M-4K	Classifier grind mill	100M	4000
LG-100M-3K	Classifier grind mill	100M	3000
LG-100M-2K	Classifier grind mill	100M	2000

Lactose 100M was jet milled at the pressures of 3 and 5 bars and at various classifying wheel speeds. The resulting lactose powders were noted as LJ-100M. The experimental conditions for jet milled coarse particle are listed in Table 2.

2.2. *Size determination*

Particle size distribution was determined using a laser diffraction particle sizer (Coulter LS 230, Coulter Corporation, Hialeah, FL, USA), equipped with a small volume module. Powders were sonicated in isopropyl alcohol (IPA) for 0.5 min to break the agglomerates before measurement, following an earlier study [26]. The $D_{v(10)}$, $D_{v(50)}$ and $D_{v(90)}$ values (representing the 10th, 50th and 90th percentiles of the cumulative size plot, respectively) of the samples were determined. The spread of the size distribution was represented by the span $[(D_{v(90)} - D_{v(10)}/D_{v(50)}]$, where a larger span value indicates a broader size distribution.

2.3. *Shape and surface morphology determination*

Shape and surface morphology were examined using scanning electron microscopy (SEM). SEM photomicrographs were captured using the Phenom SEM (FEI, Hillsboro, OR, USA) without coating. The shape of particles was expressed using aspect ratio, a quotient of the length to width.

2.4. *Tapped density determination*

Each powder was transferred into a graduated cylinder with an exact volume of 10 mL and excess powder was removed with a spatula. The tapped density was measured by tapping the powder using a Tap Density Tester (TD 2, SOTAX Corporation, Hopkinton, MA, USA). Tapped density value of the powder was

Table 2 – Parameters for producing the jet-milled coarse particles.

Batch	Mesh	Classifier speed (rpm)	Pressure (bar)
LJ-100M-4K-3b	100	4000	3
LJ-100M-4K-5b	100	4000	5
LJ-100M-3K-3b	100	3000	3
LJ-100M-3K-5b	100	3000	5
LJ-100M-2K-3b	100	2000	3
LJ-100M-2K-5b	100	2000	5

calculated from the weight and the final volume of the powder. The measurements were performed in triplicate.

2.5. X-ray diffraction

To monitor the phase purity of lactose manufactured under different conditions, the feed materials and milled samples were analyzed using powder X-ray diffraction (PXRD) with Cu K_α radiation (XRD 2000, Shimadzu, Kyoto, Japan). The 2θ range of the scan was 2–55° with a step size of 0.02° and a dwell time of 5 s.

2.6. Roughness measurement

For each batch, 60 particles were randomly selected and analyzed using optical profiler (Wyko NT1100, Veeco, Tucson, AZ, USA). Surface roughness of the carrier particles was analyzed under a field of view of 109.7 μm × 144.1 μm. Surface roughness was quantified using the arithmetic mean roughness (R_a) calculated from an area of 20 μm × 20 μm using Vision 3.0 software (Veeco, Tucson, AZ, USA). The small area for roughness measurement was necessitated by the limited surface area of each particle. The area for roughness measurement was adjusted for particles smaller than 20 μm.

2.7. Fracture strength measurement

A Nanoscope IIIa Multimode AFM (Veeco Metrology Group, Santa Barbara, CA) was used to test the fracture strength for different sides (side 1 and side 2 in Fig. 1A) of sieved (20–100 μm) individual Pharmatose 100M particles. The narrower side of lactose particle is side 2 while the wider side is side 1. The identification of side was aided by the optical microscopy on the indentor. The experiments were performed on at least 100 individual particles at 25 °C and 50% RH using a procedure similar to that reported elsewhere [27]. The load that fractured the particle was recorded. The conditions were: 25 nm/s surface approach velocity, time to load of 30 s, surface approach distance of 1000 nm, allowable drift rate of 0.5 nm/s, and the maximum load of 500 mN.

2.8. Data analysis

Statistical analysis between different batches was carried out using the Student's t-test at a P-value of 0.05 using a statistical package (Minitab, Version 15.1.0.0, Minitab Inc., USA).

3. Results and discussion

3.1. Particle size, shape, and tapped density

Sieved, classified, and classified grind milled lactoses were all tabular (Fig. 1). Surprisingly, jet milled lactose particles were slab-like (Fig. 1D) and each individual lactose particle presented two different cross-section profiles. One side appeared tabular while the other was more needle-like. For the tabular section, the aspect ratio was in the region of about 1.5 whereas the needle-shape section had an aspect ratio of 3–5. Particle

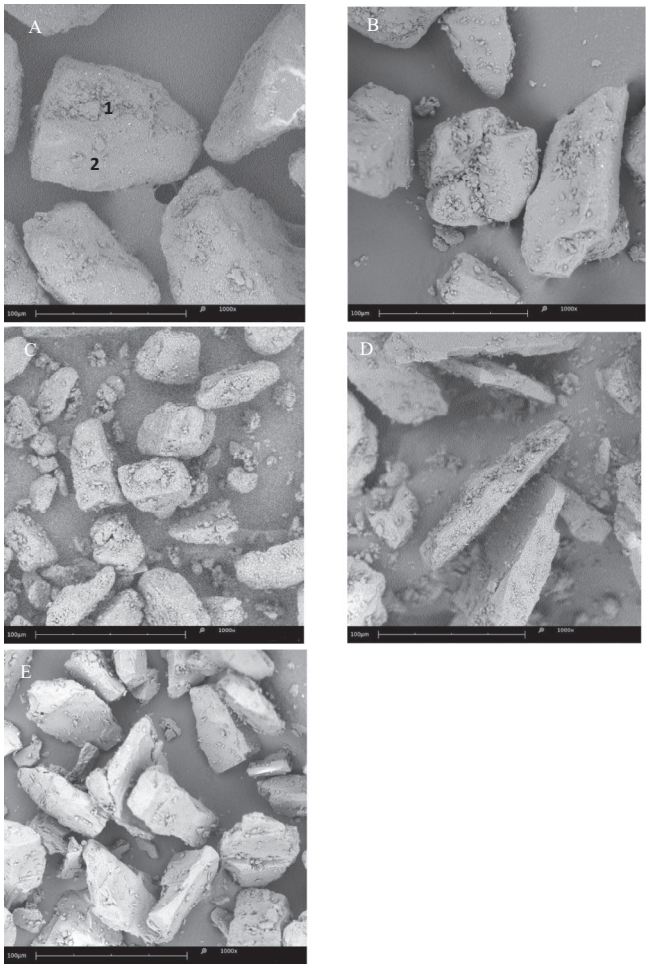

Fig. 1 – SEM photomicrographs of lactose particles using process: (A) sieved; (B) classified; (C) classified grind milled; (D) jet milled; (E) jet milled lactose at 3000 rpm classifier speed. The scale bar is 100 μm.

size, shape, and tapped density for all batches are listed in Tables 3 and 4. The coarse particles were in the size range of 8–100 μm.

For classified lactose, with and without milling (LG-100M and LC-100M in Table 3, respectively), higher classifying speed corresponded to smaller particle size as expected (Table 3). This is because a higher rotational speed exerted a greater centrifugal force allowing only smaller, lighter lactose particles to

Table 3 – Size, shape and tapped density results for conventional particles.

Batch	Size		Aspect ratio	Tapped density (g/ml)
	$D_{v(50)}$ (μm)	Span		
LA-100M	65.4 ± 2.54	1.31	1.50 ± 0.67	0.65 ± 0.02
LC-100M-4K	15.9 ± 1.67	2.41	1.40 ± 0.31	0.63 ± 0.02
LC-100M-3K	23.2 ± 1.55	2.52	1.43 ± 0.21	0.69 ± 0.02
LC-100M-2K	54.8 ± 1.20	2.01	1.39 ± 0.19	0.64 ± 0.01
LG-100M-4K	16.1 ± 1.32	2.33	1.21 ± 0.16	0.64 ± 0.02
LG-100M-3K	27.1 ± 1.34	2.15	1.33 ± 0.27	0.65 ± 0.02
LG-100M-2K	46.8 ± 1.98	2.31	1.29 ± 0.15	0.62 ± 0.01

Table 4 – Size, shape and tapped density results for jet milled coarse particle.

Batch	Size		Aspect ratio	Tapped density (g/ml)
	$D_{v(50)}$ (μm)	Span		
LJ-100M-4K-3b	41.03 ± 3.13	2.19	1.47 ± 0.02	0.54 ± 0.03
LJ-100M-4K-5b	30.72 ± 5.62	1.97	1.45 ± 0.01	0.55 ± 0.04
LJ-100M-3K-3b	18.09 ± 2.31	2.38	1.53 ± 0.04	0.54 ± 0.06
LJ-100M-3K-5b	12.12 ± 2.46	2.21	1.53 ± 0.01	0.61 ± 0.04
LJ-100M-2K-3b	10.33 ± 3.45	2.26	1.53 ± 0.01	0.61 ± 0.01
LJ-100M-2K-5b	8.097 ± 1.56	2.42	1.50 ± 0.03	0.67 ± 0.03

be carried along the air stream against the centrifugal force to pass through the vanes of the classifying wheel into the product collection bin. Classified particles (LC-100M) and classified grind milled particles (LG-100M) had the same tapped density as sieved particles (LA-100M) (Table 3).

The median particle size of the coarse jet milled lactose (Table 4, LJ-100M) was smaller but the size distribution was wider compared with sieved lactose particles (Table 3, LC-100M). As expected, higher jet milling air pressure resulted in smaller particles (Table 4, LJ-100M-4K-5b, 100M-3K-5b, 100M-2K-5b) because of the higher particle–particle collision velocity induced by the higher air pressure. The tap density of jet milled particles (Table 4, LJ-100M) was lower than sieved (Table 3, LA-100M) and classified particles (Table 3, LC-100M). This can be explained by the less efficient packing of the slab-like particles than the sieved tomahawk particles.

The shape values of jet milled lactose particles varied with classifying wheel speed (Table 4). Smaller particles collected using a higher classifying wheel speed were more uniform in size and appeared rounder [28]. More slab-like particles were obtained at the classifier wheel speed of 3000 rpm (LJ-100M-4K-3b, LJ-100M-3K-3b, LJ-100M-2K-3b), as indicated by aspect ratio shown in Table 4. This also occurs for classified grind milled coarse lactose (LG-100M-3K). It is attributed to the retention time of the particles in the milling chamber determined by the classifier wheel speed. The preset classifier wheel speed determines which size of particles can pass through. A higher classifier wheel speed generates a greater centrifugal force allowing only smaller particles to pass through; whereas a lower speed generates a lower centrifugal force allowing bigger particles to pass through. Hence, the product using a lower classifier wheel speed will be experiencing shorter fracture period. On the other hand, it would require longer time to mill down the particles to the required smaller size when the classifying wheel speed was higher. Therefore, an optimal wheel speed needs to be identified to produce more slab-like particles. A shorter residence time might not be enough for complete fracture required for forming slab-like particles. On the other hand, a longer residence time led to extensive particle attrition and, hence, rounder particles were obtained. In either case, the proportion of slab like particle was lower than the 3000 rpm wheel speed. Jet milled particles (Table 4, LJ-100M) had slightly higher aspect ratio value than the sieved particles (Table 3, LC-100M) ($P > 0.05$). However, it should be noted the aspect ratio is a simplistic two-dimensional parameter and thus cannot fully describe the 3-dimensional shape of the jet milled lactose, which is an elongated slab as discussed earlier (Fig. 1D).

3.2. *Surface roughness*

The surface for sieved lactose without fines was relatively flat and smooth with very few crevices and protrusions (Fig. 2A). The R_a was 185.44 ± 54.81 nm. By comparison, the R_a of jet milled coarse carrier was 328.02 ± 100.76 nm (Fig. 2B) which is significantly rougher than that of sieved coarse carrier ($P < 0.05$). The higher roughness of jet milled particles is likely a result of random impact between particles during jet milling and imperfect propagation of cracks along crystallographic planes.

3.3. *Crystallinity*

It is known that crystallinity generally reduces when a prolonged milling is employed [29–34]. However, jet milled coarse carriers in this study remained highly crystalline as shown by PXRD data (Fig. 3). This may be attributed to the short resident time in the milling chamber.

3.4. *Fracture strength test and collision hypothesis*

The fracture strength of single lactose particle (Fig. 1A) was 0.072 MPa for side 1 and 0.175 MPa for side 2, which is similar to a previous report [27]. The difference in fracture strength of different sides was also reported elsewhere [35]. Similarly, it was found that the broad flat side of the jet-milled particles had the higher fracture strength than the narrow elongated sides. Thus, cracks will be more easily generated when the weaker side of the lactose crystal was impacted during collision between particles. The slab-like appearance of the milled lactose particles was brought about by this mode of attrition during milling. The air flow also tended to orientate particles with their longest face along the direction of airflow; hence collision more likely occurred between the narrow sides of neighboring particles. Moreover, cracks more readily propagated along this direction to become parallel to the axial direction of the compressive stress. These cracks propagated and started to interact with neighboring cracks inside of the particle, thus brought about crack coalescence and finally, macroscopic particle fractured [36]. Therefore, the narrower face would be sliced broken to result in slab-shape lactose particles. The step-wise formation mechanism of the slab-like lactose particles is illustrated in Fig. 4.

4. Conclusions

A new type of slab-like lactose particles was produced by jet-milling. Bulk powders of this carrier particle type in the range of 8–45 μm were obtained by controlled jet milling. Production of slab-like particles depends on the particle retention time in the milling chamber. Optimal retention time is needed for complete fracture of lactose particles to occur. A higher classifier wheel speed resulted in a shorter retention time while a lower classifier wheel speed led to a longer retention time. The optimal conditions involve a classifier wheel speed of 3000 rpm during jet milling, which corresponded to the production of a relatively higher amount of slab-like particles in the milled product. The newly obtained

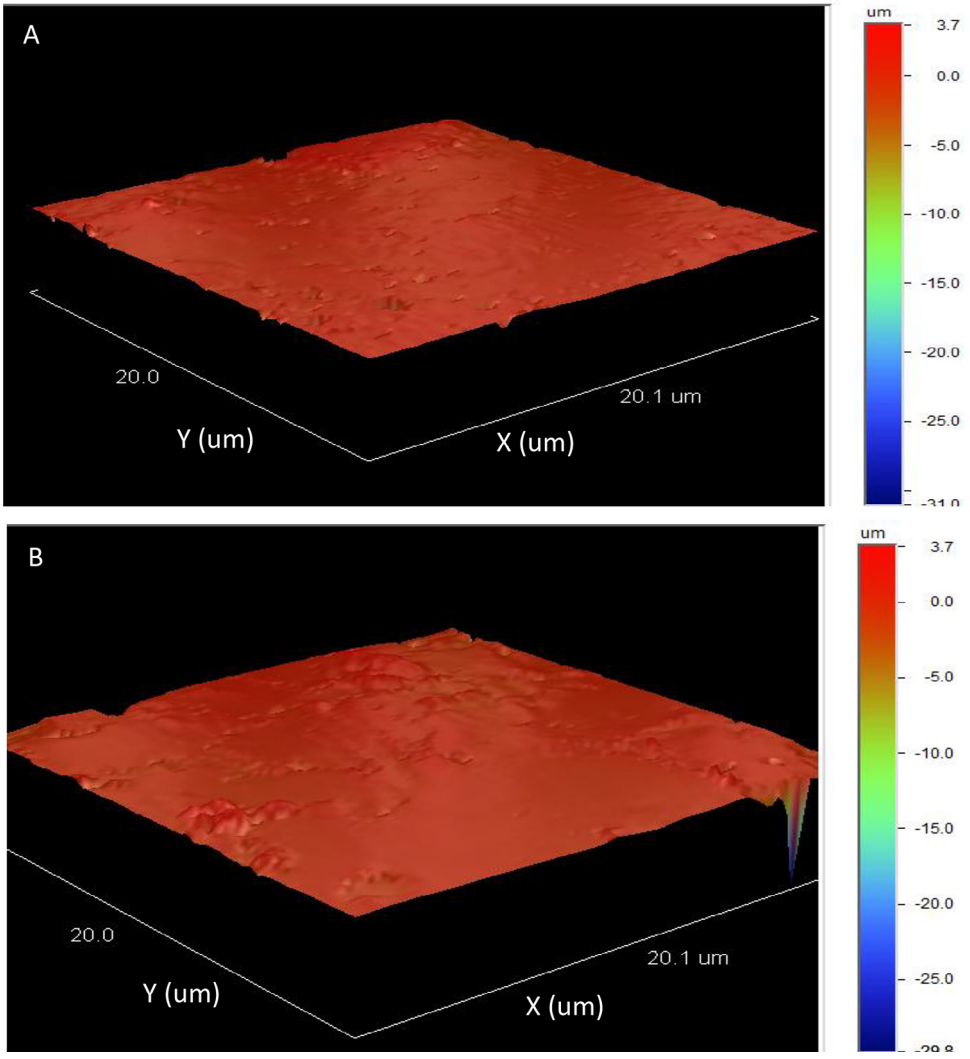

Fig. 2 – Surface roughness of (A) sieved coarse carrier and (B) jet milled coarse carrier.

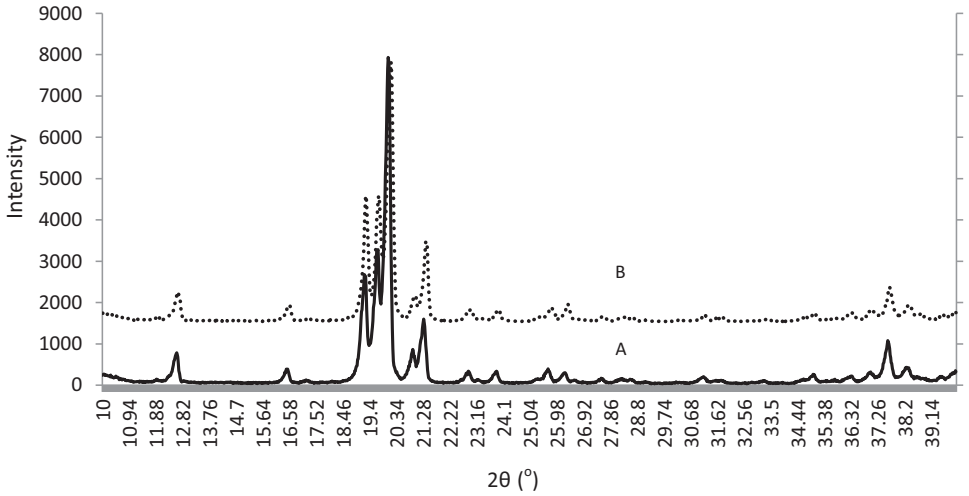

Fig. 3 – PXRD for (A) raw lactose and (B) jet milled lactose.

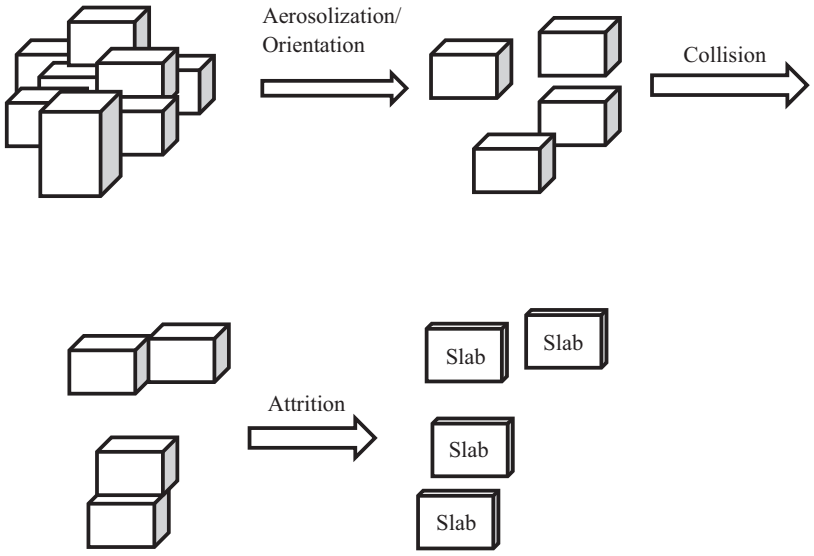

Fig. 4 – Illustration of slab-like particle formation.

slab-shaped particle has potential application in dry powder inhaler formulation where powder property is critical in final product performance.

Acknowledgements

The authors would like to thank the funding support for this study from GEA-NUS PPRL (N-148-000-008-001) and SERC Grant No. 102 169 0049 (R-148-000-157-305). Xiang Kou was a recipient of the National University of Singapore Graduate Research Scholarship. Some of the experiments were performed at the University of Minnesota I.T. Characterization Facility, which receives partial support from the NSF through the NNIN program.

REFERENCES

[1] Kou X, Chan LW, Steckel H, et al. Physico-chemical aspects of lactose for inhalation. Adv Drug Deliv Rev 2012;64:220–232.
[2] Steckel H, Müller BW. In vitro evaluation of dry powder inhalers II: influence of carrier particle size and concentration on in vitro deposition. Int J Pharm 1997;154:31–37.
[3] Fu X, Huck D, Makein L, et al. Effect of particle shape and size on flow properties of lactose powders. Particuology 2012;10:203–208.
[4] Kaialy W, Alhalaweh A, Velaga SP, et al. Effect of carrier particle shape on dry powder inhaler performance. Int J Pharm 2011;421:12–23.
[5] Crowder TM, Rosati JA, Schroeter JD, et al. Fundamental effects of particle morphology on lung delivery: predictions of Stokes' law and the particular relevance to dry powder inhaler formulation and development. Pharm Res 2002;19:239–245.
[6] Dickhoff BHJ, de Boer AH, Lambregts D, et al. The interaction between carrier rugosity and carrier payload, and its effect on drug particle redispersion from adhesive mixtures during inhalation. Eur J Pharm Biopharm 2005;59:197–205.
[7] Wan J, Wang XZ, Ma CY. Particle shape manipulation and optimization in cooling crystallization involving multiple crystal morphological forms. AIChE J 2009;55:2049–2061.
[8] Liu JJ, Hu YD, Wang XZ. Optimization and control of crystal shape and size in protein crystallization process. Comput Chem Eng 2013;57:133–140.
[9] Lovette MA, Doherty MF. Needle-shaped crystals: causality and solvent selection guidance based on periodic bond chains. Cryst Growth Des 2013;13:3341–3352.
[10] Zeng XM, Martin GP, Marriot C, et al. Lactose as a carrier in dry powder formulations: the influence of surface characteristics on drug delivery. J Pharm Sci 2001;90:1424–1434.
[11] Zeng XM, Martin GP, Marriott C, et al. The use of lactose recrystallised from carbopol gels as a carrier for aerosolised salbutamol sulphate. Eur J Pharm Biopharm 2001;51:55–62.
[12] Larhrib H, Martin GP, Marriott C, et al. The influence of carrier and drug morphology on drug delivery from dry powder formulations. Int J Pharm 2003;257:283–296.
[13] Larhrib H, Martin GP, Prime D, et al. Characterisation and deposition studies of engineered lactose crystals with potential for use as a carrier for aerosolised salbutamol sulfate from dry powder inhalers. Eur J Pharm Sci 2003;19:211–221.
[14] Kaialy W, Momin MN, Ticehurst MD, et al. Engineered mannitol as an alternative carrier to enhance deep lung penetration of salbutamol sulphate from dry powder inhaler. Colloids Surf B Biointerfaces 2013;79:345–356.
[15] Kaialy W, Martin GP, Ticehurst MD, et al. The enhanced aerosol performance of salbutamol from dry powders containing engineered mannitol as excipient. Int J Pharm 2010;392:178–188.
[16] Lovette MA, Muratore M, Doherty MF. Crystal shape modification through cycles of dissolution and growth: attainable regions and experimental validation. AIChE J 2012;58:1465–1474.
[17] Kwon OP, Kwon S-J, Jazbinsek M, et al. Morphology and polymorphism control of organic polyene crystals by tailor-made auxiliaries. Cryst Growth Des 2006;6:2327–2332.
[18] Weissbuch I, Popovitz-Biro R, Lahav M, et al. Understanding and control of nucleation, growth, habit, dissolution and structure of two- and three-dimensional crystals using 'tailor-made' auxiliaries. Acta Crystallogr B 1995;51:115–148.

[19] Weissbuch I, Lahav M, Leiserowitz L. Toward stereochemical control, monitoring, and understanding of crystal nucleation. Cryst Growth Des 2003;3:125–150.
[20] Abbas A, Srour M, Tang P, et al. Sonocrystallisation of sodium chloride particles for inhalation. Chem Eng Sci 2007;62:2445–2453.
[21] Dhumal R, Biradar S, Paradkar A, et al. Ultrasound assisted engineering of lactose crystals. Pharm Res 2008;25:2835–2844.
[22] Dhumal RS, Biradar SV, Paradkar AR, et al. Particle engineering using sonocrystallization: salbutamol sulphate for pulmonary delivery. Int J Pharm 2009;368:129–137.
[23] Pitchayajittipong C, Shur J, Price R. Engineering of crystalline combination inhalation particles of a long-acting β2-agonist and a corticosteroid. Pharm Res 2009;26:2657–2666.
[24] Parmar MM, Khan O, Seton L, et al. Polymorph Selection with Morphology Control Using Solvents. Cryst Growth Des 2007;7:1635–1642.
[25] Young PM, Cocconi D, Colombo P, et al. Characterization of a surface modified dry powder inhalation carrier prepared by "particle smoothing". J Pharm Pharmacol 2002;54:1339–1344.
[26] Adi H, Larson I, Stewart P. Laser diffraction particle sizing of cohesive lactose powders. Powder Technol 2007;179:90–94.
[27] Masterson VM, Cao X. Evaluating particle hardness of pharmaceutical solids using AFM nanoindentation. Int J Pharm 2008;362:163–171.
[28] Chan LW, Lee CC, Heng PWS. Ultrafine grinding using a fluidized bed opposed jet mill: effects of feed load and rotational speed of classifier wheel on particle shape. Drug Dev Ind Pharm 2002;28:939–947.
[29] Florence AT, Salole EG, Stenlake JB. The effect of particle size reduction on digoxin crystal properties. J Pharm Pharmacol 1974;26:479–480.
[30] Lee KC, Hersey JA. Crystal modification of methisazone by grinding. J Pharm Pharmacol 1979;29:249–250.
[31] Chattoraj S, Bhugra C, Telang C, et al. Origin of two modes of non-isothermal crystallization of glasses produced by milling. Pharm Res 2012;29:1020–1032.
[32] Listiohadi YD, Hourigan JA, Sleigh RW, et al. Effect of milling on the caking behavior of lactose. Aust J Dairy Technol 2005;60:214–224.
[33] Kwan CC, Chen YQ, Ding YL, et al. Development of a novel approach towards predicting the milling behaviour of pharmaceutical powders. Eur J Pharm Sci 2004;23:327–336.
[34] Qiu Z, Stowell JG, Cao W, et al. Effect of milling and compression on the solid-state Maillard reaction. J Pharm Sci 2005;94:2568–2580.
[35] Hassanpour A, Ghadiri M, Bentham AC, et al. Distinct element analysis of the effect of temperature on the bulk crushing of lactose monohydrate. Adv Powder Technol 2003;14:427–434.
[36] Wong RHC, Chau KT, Tang CA, et al. Analysis of crack coalescence in rock like materials containing three flaws – part 1: experimental approach. Int J Rock Mech Min Sci 2001;38:909–924.